Egypt. J. Chem. **Vol. 64,** No. 10 pp. 6053 - 6066 (2021)

Egyptian Journal of Chemistry

http://ejchem.journals.ekb.eg/

Synthesis and evaluation of poly (Indole/Thiophene) fused ring derivative for C- steel corrosion inhibitor in sulfuric acidic medium

Asmaa A. I. Ali[a], Rasha A. Baseer[b*], Heba M. Abo-Salem[c], S.M. Syam[a]

[a]*Physical Chemistry Department, Faculty of Science, Benha University, Postal code. 13518- Benha, Egypt*

[b]*Department of Polymers and Pigments, Chemical Industries Research Division, National Research Centre; Postal code.12622- Dokki- Giza- Egypt.*

[c]*Department of Natural Compounds, Pharmaceutical Industries Research division, National Research Centre, Postal code 12622- Dokki-Giza- Egypt*

Abstract

The current study aims to explore the anti-corrosion performance of Poly [2-amino-4(1-benzyl-1H-indol-3-yl) thiophene -3-carbonitrile)] (PABITC) on C-steel in in 0.50 M H2SO4 using weight loss and potentiodynamic polarization measurements (PDP).. PABITC was synthesized with different molecular weights 882, 921, 1388, 15788 g/mol using APS as an oxidizing agent. The chemical structure of the polymer was characterized using H1NMR, DNMR, C13NMR, and FTIR spectroscopy . Polarization results reveal that the synthesized polymer acts as a hybrid-type inhibitor. The adsorption of inhibitory atoms of the polymer on the C- steel surface followed Langmuir isotherm. SEM and EDX assure the development of PABITC adsorbed film on the C- steel surface. Quantum calculations were carried out to elucidate the reactive sites in PABITC. All the results approve that PABITC makes a resistive layer to shrink the corrosion process.

Keywords: Poly(2-amino-4(1-benzyl-1H-indol-3-yl)thiophene-3-carbonitrile); C- steel; Corrosion inhibition

1. Introduction

In recent decades, C-steel has been among the most significant material in the industry for its high mechanical strength, high reinforcement, and lower cost. It has been used for various applications such as chemical processing, petroleum industry, construction, transportation, electronics, and medical applications [1, 2].

C- steel has been affected mainly by corrosion that occurs by chemical and electrochemical reactions [3, 4]. Many approaches to minimizing the corrosion impact, such as inhibitors, electrochemical protective techniques, metallic and non-metallic protective coating, have been considered [5]. Organic inhibitors are the most practical and cost -effective ways for improving metallic performance.

In many cases, fluid is the most practical media for inhibitors application where the inhibitors act through some mechanisms of adsorptions [6, 7]. Therefore, the inhibitors standing up a barrier between the metal surface and corrosive media [7]. It is known that most organic compounds that primarily contain atoms of nitrogen, sulfur, or oxygen in their molecular backbone are usually acted as acid inhibitors, attributing interaction with C-steel surface via adsorption [8, 9].

Several factors affect the adsorption behavior, such as the metal's nature and its surface voltage, the inhibitor's chemical composition, the form of a corrosive medium, and the corrosion reaction temperature. Both chemical- and physical-sorption are primarily the interaction mechanisms of the inhibitor-metal at the interface [10].

The organic molecules' adsorption on the metal surface attributes to their electron-donating ability that relating to the presence of π-orbitals, aromaticity, and functional groups such as amines and carbonitrile, which reveal high performance in corrosion inhibition [1, 11-14]. Adsorption of such inhibitors could be further explained through four mechanisms [15]; electrostatic interaction between the charged metal surface and the charged inhibitor, interaction of electron lone-pairs in the inhibitor with the metal, interaction of p-electrons of the inhibitor with the metal, or a blend of the three preceding forms.

In other words, the adsorption at the metal surfaces of these organic inhibitors may induce bond formation between the unshared electron pairs from their donor atoms and metal orbitals. It contributes to the eventual film formation, thereby preventing the flow of corrosive ions and

*Corresponding author e-mail: ra.abdelbasser@nrc.sci.eg, rasha.daaader@gmail.com

Receive Date: 07 June 2021, Revise Date: 28 July 2021, Accept Date: 01 August 2021

DOI: 10.21608/EJCHEM.2021.79610.3914

molecules to the metal surface, and that inhibits the corrosion [16].

Over the last three decades, conductive polymers such as polyaniline, polypyrrole, polyindole, and polythiophene have taken great care to protect mild steel from corrosion [14, 17, 18].The most common technique of the conductive polymers in corrosion protection is the formulation of paint or coating film [19-23] Copolymerization is the best way to improve conductive polymers' inhibition efficiency [24-27].

Our scope in this research is to synthesize and evaluate a new polymer based on the fused ring between Indole and Thiophene rings. The copolymer of the Indole / Thiophene reflects an identical image of a uniform molecular arrangement that equally distributes the charges, hence increases the polymer's inhibition efficiency. In addition, the synthesized polymer contains amine and carbonitrile groups that exhibit high inhibition efficiency towards C-steel corrosion[1, 23].

The corrosion performance for steel was evaluated utilizing potentiodynamic polarization and weight loss techniques. Experiments were performed at room temperature as a function of concentrations. Moreover, quantum parameters were employed by the density functional theory (DFT) method to prove the experimental results. Where it enhanced a more reliable perception of the interaction mechanism between the inhibitor molecule and the iron surface. SEM and EDX were performed after corrosion in the absence and presence of optimal concentrations of PABITC. Those analyses can provide more useful information about the efficacy of protective and/or corrosion inhibiting treatment.

2. Experimental

2.1. ***Materials***

1-(1-benzyl-1H-indol-3-yl) ethanone, were purchased from Merck Company. The other reagents and solvents were of commercial grade.

C- Steel specimens having composition: (wt. %): C= 0.38-0.45, Cr = 0.90-1.20, Mo = 0.15-0.25, Si = 0.17-0.37, Mn = 0.50-0.80, Fe = rest were used for weight loss and the electrochemical corrosion tests. The tested C-steel was previously worked in the Cairo.Co. for petroleum pipelines' transportation.

The aggressive solution of 0.50 M H_2SO_4 was prepared by diluting the analytical grade, Merck, 98 % H_2SO_4 with bi-distilled water. Various concentrations (0.01–1.0 mM) of the synthesized PABITC were also prepared in bi-distilled water and used as inhibitors for C- steel corrosion in 0.50 M H_2SO_4**.**

2.2. Methods

2.2a. *Synthesis of [2-amino-4(1-benzyl-1H-indol-3-yl) thiophene-3-carbonitrile)] (ABITC)*

ABITC was prepared as reported in the literature [28] via Gewald reaction. *N*-benzyl-3-acetyl indole was prepared as reported in the literature[29]. To a solution of 2-(1-(1-benzyl-1*H*-indol-3-yl) ethylidene) malononitrile (**B**, 0.05 mol) and sulfur (1.6 g, 0.05 mol) in absolute ethanol (50 ml), diethylamine (3.65 g, 0.05 mol) was added dropwise at 15 ºC, and the reaction mixture was then stirred at 65 ºC for 2 h. After all, the solvent was evaporated, the residue was dissolved in absolute ethanol (50 mL) followed by further stirring in an ice bath for 30 min. The solid that formed was filtered off, washed with water, air-dried, and crystallized from methanol. IR 3102 & 3035 (NH2), 2207 (CN) and 1640 (C=C). H1NMR (400MHz, DMSO-d6) 8.56 (1H, s, H-2 ind.), 8.23 (1H, s, H-5 thiophene), 7.55 (2H, s, NH2), 7.35-7.19 (9H, m, Ar-H) and 5.51 (2H, s, CH2-N). The spectral data agreed with the previously reported data of ABITC.

2.2b. *Synthesis of poly(2-amino-4-(1-benzyl-1H-indol-3-yl) thiophene-3-carbonitrile) (PABITC)*

A solution of APS was wisely added to 2-amino-4-(1-benzyl-1H-indol-3-yl) thiophene-3-carbonitrile solution supported by homogenization for 10 min. The solution was then sonicated for 10 min, Power 40%. Finally, the solution was refluxed 2 h later with pouring ethylene glycol for Mw controlling. The mixture was poured into ethanol (500 ml) and then stirred for another 2 h to remove the reactants. Polymer eventually separated in a greasy form using a separating funnel and washed with ethanol several times and dried at 60 ℃ for 24 h.

2.3. Gravimetric experiment

A rectangular design of the 1.6 cm, 1.5 cm or 0.7 cm test specimens was abraded with a series of emery paper (grade 320–400–600–800–1000–1200), subsequently washed with bi-distilled water, ethanol and acetone and eventually dried in dry air before use. Each sample was accurately weighed then the samples were immersed in 100 mL of 0.50 M H_2SO_4, with different concentration of the poly (2-amino-4-(1-benzyl-1H-indol-3-yl) thiophene-3-carbonitrile) for 12 h. After the period elapsed the corrosion products have been removed [30], and the samples were thoroughly rinsed with bi-distilled water, dried, and weighed with precision. Each experiment was performed three times, and its

average values were recorded. The corrosion rates (***CR***) were calculated from the equation **[1]**:

$$\boldsymbol{CR_W = \frac{W}{St}} \qquad [\mathbf{1}]$$

where $\boldsymbol{W}$ is the average loss in weight **(g)**, $\boldsymbol{S}$ is surface area (cm^2) of the worked specimen and $\boldsymbol{t}$ is the exposure time (**h**). The inhibition efficiencies (***IE***) were evaluated according to equation **[2]**, where $\boldsymbol{CR_{W^o}}$ and $\boldsymbol{CR_W}$ are the corrosion rates in the absence and presence of the inhibitor, respectively.

$$\boldsymbol{IE_{(W)} = \frac{CR_{W^o} - CR_W}{CR_{W^o}} \times 100} \qquad [\mathbf{2}]$$

The degree of the surface coverage of inhibitor molecules at the metal surface were determined from $\boldsymbol{IE_{(W)}}$ according to the following equation **[3]**:

$$\boldsymbol{\theta = \frac{CR_{W^o} - CR_W}{CR_{W^o}}} \qquad [\mathbf{3}]$$

The corrosion tests were performed without stirring the solutions. The solutions temperature was controlled thermostatically at 25 ± 1 °C.

2.4. Electrochemical measurements

Three Water electrodes-jacketed electrochemical cell model consisted of a reference electrode Ag/ AgCl (3.0 M), a platinum foil counter electrode, and a C-steel cylinder encapsulated as a working electrode in epoxy resin with 0.50 cm^2 was used. All the electrochemical experiments were performed using 50 mL of electrolyte. The electrolyte was 0.5 M H_2SO_4 free and with the addition of different concentrations of the series of PABITC. Experiments were performed as a function of concentration by using 0.01, 0.1, 0.3 and 1.0 mM PABITC. The electrochemical measurements were carried out using A PGSTAT 302N (Metrohm Autolab) potentiostat/galvanostat. The open-circuit potential (OCP) was stabilized for 30 min before the electrochemical tests. Potentiodynamic polarization curves were acquired in the potential window ranging from -150 to + 150 mV vs OCP at a scan rate of 1.0 mV / s to determine kinetic parameters and corrosion inhibition efficiency. The inhibition efficiency $\mathbf{IE_{PDP}}$ was estimated according to equation **[4] [31]**:

$$\mathbf{IE_{PDP} = \frac{I^o_{Corr} - I_{Corr}}{I^o_{Corr}} \times 100} \qquad [\mathbf{4}]$$

Where $\mathbf{I^o_{Corr}}$, $\mathbf{I_{Corr}}$ is the corrosion current densities in the absence and presence of (**PABITC**), respectively.

2.5. Surface morphological analysis

Scanning electron microscope (SEM) and energy dispersive X- ray spectroscopy (EDX) (JEM-1230, Japan) have been employed to indicate the Morphological properties and chemical analysis of the C- steel surface after the corrosion test. The examined samples were: C- steel specimen immersed in 0.50 M H_2SO_4 in the absence and presence of 1.0 x10 $^{-3}$ M inhibitors (P1, P3, and P4).

2.6. Quantum chemical calculations

A theoretical study was carried out to explore the significant active sites of the PABITC molecule and make clear its possible interplay with the iron surface. The quantum chemical calculations of PABITC were performed by using DMOL [32] modulus which is designed based on density function theory (DFT) in the material studio package. DFT semi-core pseudopods calculation has been carried out with double numerical basis sets plus polarization functional (DNP) that are of similar quality to 6-31 G Gaussian basis sets. All quantum chemical parameters have been derived primarily based on the electronic parameters of the most stable conformers of the molecule. The frontier molecular orbital energies, that is, the highest occupied molecular orbital energy (E_{HOMO}) and the lowest unoccupied molecular orbital energy (E_{LUMO}) had been calculated. Other parameters such as the energy gap (ΔE), global hardness (η), the inverse value of global hardness (σ) electronegativity (χ), and the fraction of electrons transfer (ΔN) according to the equations **[5-8]** [33-35]:

$$\boldsymbol{\Delta E = E_{LUMO} - E_{HOMO}} \qquad [\mathbf{5}]$$

$$\boldsymbol{\eta = \frac{1}{2}\left(E_{LUMO} - E_{HOMO}\right)} \qquad [\mathbf{6}]$$

$$\boldsymbol{\chi = -\frac{1}{2}\left(E_{LUMO} + E_{HOMO}\right)} \qquad [\mathbf{7}]$$

$$\boldsymbol{\Delta N = \frac{(\chi_{Fe} - \chi_{inh})}{2(\eta_{Fe} + \eta_{inh})}} \qquad [\mathbf{8}]$$

where $\boldsymbol{\chi_{Fe}}$, $\boldsymbol{\chi_{inh}}$, $\boldsymbol{\eta_{Fe}}$ and $\boldsymbol{\eta_{inh}}$ denote the electronegativity and hardness of the iron and inhibitor, respectively. A value of 7 eV/mol was used for the $\boldsymbol{\chi_{Fe}}$, while $\boldsymbol{\eta_{Fe}}$ was taken as 0 eV/mol for bulk Fe atom in accordance with the Pearson's electronegativity scale [34].

The electronegativity of iron surface in the equation [8], qualified by its work-function, whilst its chemical hardness is omitted due to $\boldsymbol{\eta}$ of bulk metals is correlating to their states density reciprocal at the Fermi level, which is an exceptionally small variety [5, 36-38].

The frequency calculations were employed to confirm the interaction between a single PABITC molecule and the iron surface.

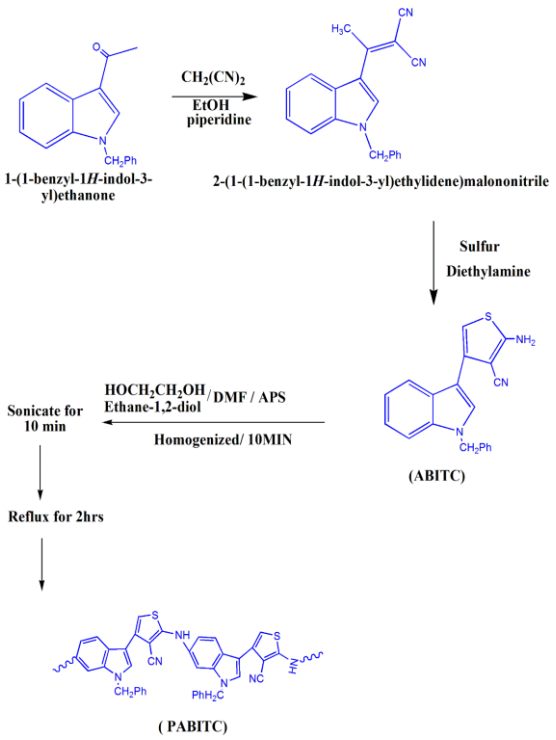

Scheme 1: Synthesis and polymerization of ABITC

3. Results and discussion

3.1. Characterization of (PABITC)

The chemical structure and the molecular weight of the synthesized PABITC were verified by ^{1}H NMR, C^{13} NMR (Bruker AVANCE 400 MHz spectrometer (Bruker) with a 5 mm BBFO probe using deuter-ated Dimethyl sulfoxide DMSO-d_6 as the solvent), FTIR (Beckman inferared spectrophotometer PU 7712 using KBr disk) and Gel permeation chromatography (Agillent 1100, Germany). Sundburg reported that the indole reactivity ring positions followed the trend 3 > 2 > 6 > 4 > 5 > 7 [39]. In addition to Sundberg`s studies, Dhanaraj Gopi et al. studied the electrochemical synthesis of poly (indole-*co*-thiophene) which agreed with those of Sundberg [40]. Based on this, and pervious study [41] we propose the mechanism for the polymer as shown in Scheme1, where the polymerization took place through the amine group substituted on the thiophene ring and the 6-c of the aromatic ring of indole ring.

The mechanism proposed has been confirmed by H^{1}NMR, DNMR, and C^{13}NMR. Where, H^{1}NMR and DNMR induce 8.57 (s, 1H, indolyl 2-H), 8.24 (s, 1H, thienyl 5-H), 2.49 (s, 2H, NH2), 7.52-7.10 (m, 9H, Ar-H) as shown in figure (1, 2). In addition, by magnifying the aromatic shift, 6C-H notes to disappear, whilemean 4C-H, 5C-H and 7C-H appear respectively in (7.53, 7.32, 7.2) as shown in figure (3) [42], 5.52 (s, 2H, CH_2-N), C^{13}NMR: 128.75-121.77 (Ar-C),110.58(CN), 39.62 (CH2) figure (4) .

FTIR polymer spectrum shows NH band at 3105cm-1. The peak observed at 2203cm-1 related to cyano group CN. The peak shown at 1638cm-1 was associated with C = C, where the peak shown at 1461cm-1 was associated with benzenoid rings. In addition, the peak revealed at 1385cm-1 related to C-N finally; the peak observed at 739cm-1 related to C-S figure (5).

The gel permission chromatography (GPC) determined the weight-average molecular weights (*M*w), where the polymer was synthesized with different *M*w as shown in table 1. It is noteworthy that increasing the molar ratio of ethylene glycol to ABITC decrease the *M*w of the produced polymer.

Table 1: Gel permeation chromatography (GPC) results.

Sample	Mw	Mn	PDI
P1	882	319	2.70
P2	921	631	1.50
P3	1388	895	1.60
P4	15788	9420	1.60

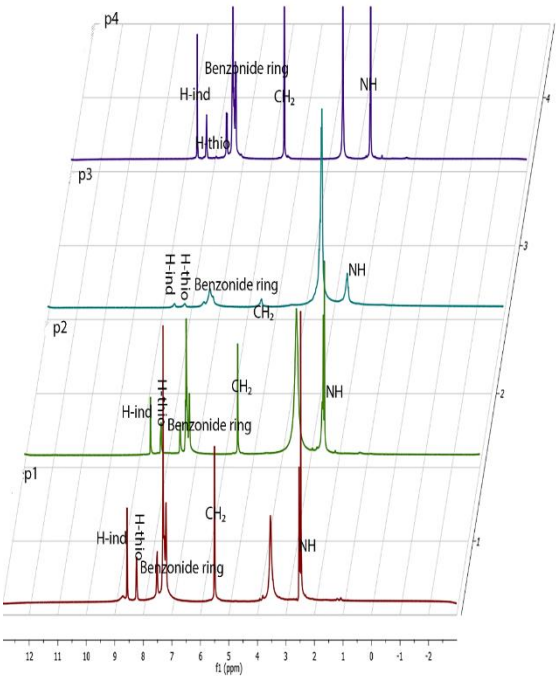

Figure1: *HNMR Spectra of poly PABITC*

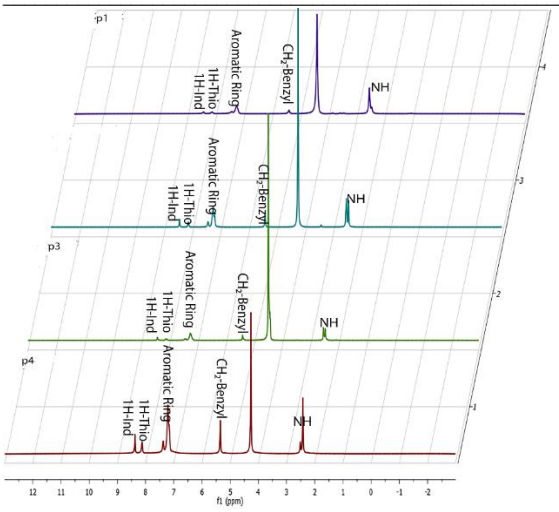

Figure 2: *DNMR Spectra of PABITC*

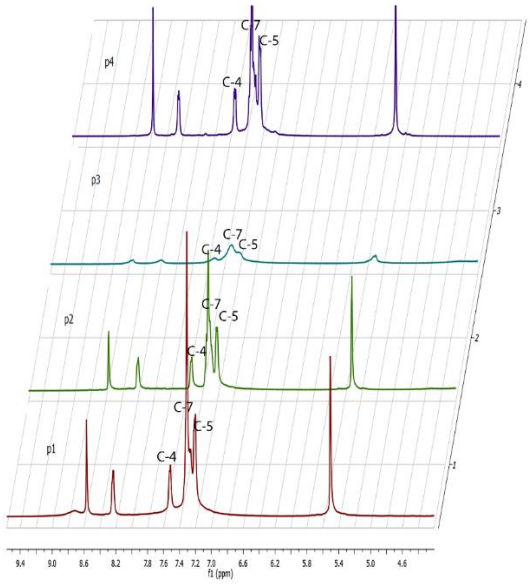

Figure 3: *Aromatic shift of PABITC in HNMR*

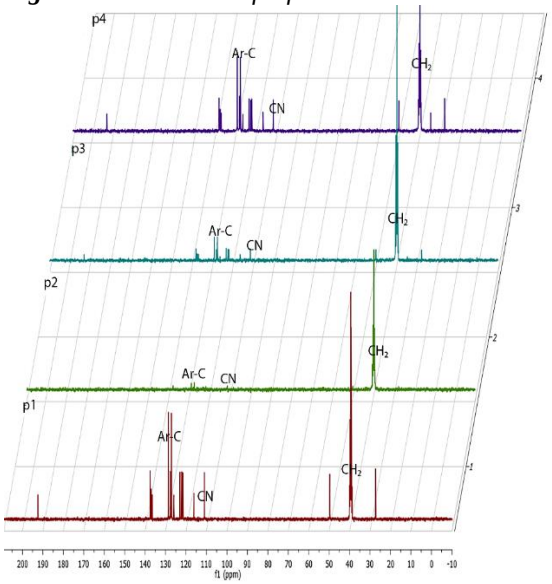

Figure 4: *C[13]NMR of PABITC*

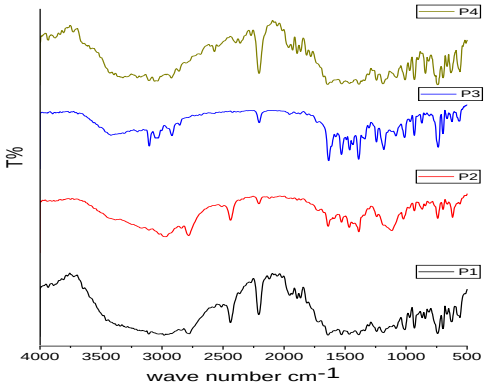

Figure 5: *FTIR spectrum of PABITC*

3.2. Weight loss measurements

The weight loss technique is the easiest procedure that indicates the impact of the inhibitor concentration on the corrosion resistance efficiency of the inhibitor. Table (2) are summarized the corrosion rates and inhibition efficiencies (*IE*%) of C- steel in 0.50 M H_2SO_4 as a function of concentrations and molecular weights for the studied PABITC. The table shows that the corrosion rate decreased sharply as the PABITC concentration increased indicating the formation of a protective PABITC layer, thus increasing the inhibition efficiencies for the different series of the PABITC. The protective PABITC layer prevents the diffusion of the corrosive species to the C- steel surface, and hence blocking their destructive effect. This behavior was imputed to the increased surface coverage adsorption of inhibitors on the C- steel as the inhibitor concentration increased. The most noteworthy corrosion resistance value of 93.75%, 95%, 97.81% and 98.7% were accomplished at 1.0 mM for the studied (P1, P2, P3 and P4) polymer respectively.

3.3. Potentiodynamic polarization measurements

Polarization curves of C-steel in 0.50 M H_2SO_4 solution containing different concentrations of the synthesized PABITC with different molecular weights (P1, P2, P3, P4) are shown in Fig. 6 (a-d) at 25 ± 1 ° C. It is clear from the figure that the decrease in current densities for both the cathodic and anodic branches with the increase in the concentration of the polymer molecules exhibits evidence for the ability of PABITC to inhibit both cathodic and anodic reactions. Fig. 6 (a-d) revealed that the corrosion potential shifted to the anodic direction with increasing the inhibitor concentration, compared to the polymer-free

solution. Hence the PABITC retarded mainly the anodic and, to some extent, the cathodic reaction.

Table 2: Corrosion parameters obtained from weight loss for carbon steel in 0.5 M H_2SO_4 in the absence and presence of PABITC series for 12 h at 298 K.

Inhibitor type		*C*, mM	*mg*/cm^2.h	*IE*%	Θ
P1		0.00	5.20	------	-----
		0.01	4.60	11.73	0.117
		0.03	3.70	29.08	0.291
		0.10	2.10	59.79	0.598
		0.30	0.40	92.81	0.928
		0.60	0.35	93.0	0.930
		1.00	0.30	93.75	0.938
P2		0.01	4.20	19.51	0.195
		0.03	3.20	38.32	0.383
		0.10	1.90	61.68	0.617
		0.30	0.30	93.33	0.933
		0.60	0.28	94.00	0.940
		1.00	0.26	95.02	0.950
P3		0.01	3.40	33.83	0.338
		0.03	2.60	50.68	0.507
		0.10	1.50	72.06	0.721
		0.30	0.20	95.63	0.956
		0.60	0.16	96.50	0.965
		1.00	0.10	97.81	0.978
P4		0.01	3.10	40.77	0.408
		0.03	1.30	75.27	0.753
		0.10	0.90	82.48	0.825
		0.30	0.10	97.80	0.978
		0.60	0.08	98.2	0.982
		1.00	0.07	98.65	0.987

The kinetic parameters were extracted from the figure and summarized in Table 3. The percentages of inhibition efficiency ***IE*%** and surface coverage Θ were calculated as reported in [31] and are displayed in Table 3.

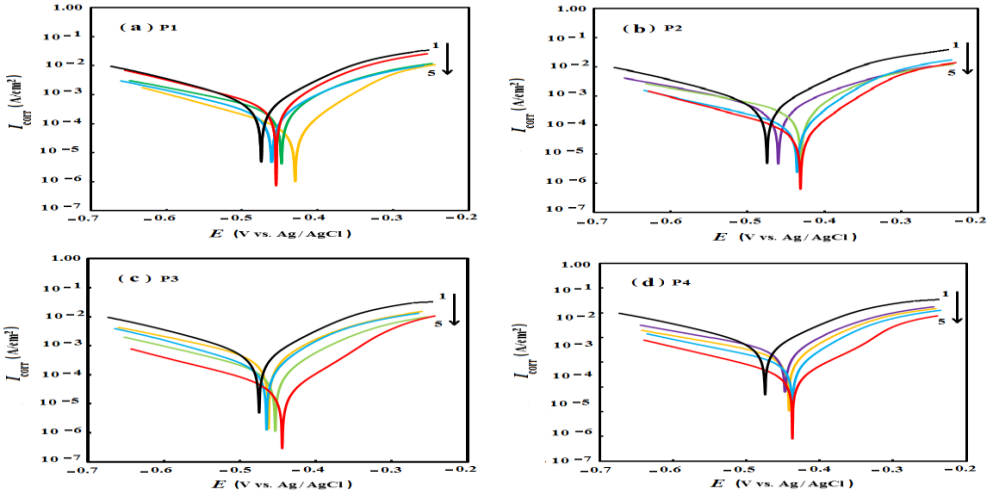

Figure 6: *Potentiodynamic polarization curves for C- steel in 0.5 M H_2SO_4 in the absence and presence of different concentrations of polymers at 298 K. (1) 0.0 M, (2) 1.0 x 10^{-5} M, (3) 1.0 x 10^{-4} M, (4) 3.0 x 10^{-4} M, (5) 1.0 x 10^{-3} M*

Table 3: Potentiodynamic polarization parameters for C- steel in 0.50 M H_2SO_4 in the absence and presence of PABITC series at 298 K.

Inhibitor type	*C*, mM	E_{corr}, V vs Ag/ AgCl	I_{corr}, µA/ cm^{-2}	βa, mV/dec	$-\beta c$, mV/dec	*IE*%	Θ
	0.00	-471.90	840.01	84.10	132.70	-----	-----
	0.01	-460.7	757.33	85.06	143.56	09.85	0.098
P1	0.10	-434.0	229.67	52.66	170.00	72.66	0.727
	0.30	-419.0	147.95	49.00	180.18	82.39	0.824
	1.00	-428.0	130.50	62.10	183.90	84.52	0.845
	0.01	-462.00	657.00	90.70	168.50	21.79	0.218
	0.10	-450.00	216.60	71.00	154.00	74.21	0.742
P2	0.30	-458.00	111.59	69.00	140.00	86.72	0.867
	1.00	-433.00	63.59	59.00	150.00	92.43	0.924
	0.01	-461.00	575.00	97.00	154.00	31.54	0.315
P3	0.10	-430.00	190.68	57.50	165.75	77.30	0.773
	0.30	-426.50	105.20	58.500	139.90	87.48	0.875
	1.00	-425.70	48.25	56.30	137.20	94.26	0.943
	0.01	-433.00	527.00	68.00	186.00	37.26	0.373
P4	0.10	-428.00	171.30	59.00	165.00	79.61	0.796
	0.30	-446.00	51.20	65.00	138.00	93.90	0.939
	1.00	-428.00	39.00	64.00	121.00	95.36	0.954

Inspection of the table demonstrates, increasing the concentration of the PABITC resulted in decreasing the corrosion current density I_{corr} ($\mu A.cm^{-2}$), increasing the inhibition efficiency (IE_{PDP}) and surface coverage (Θ). The evaluated results suggest the polymer molecules could adsorb on the C- steel surface, thus providing an increase in the surface coverage via forming a barrier film that hinders the diffusion of the corrosive medium to the metal surface. Assessment of Table 3 reveals that the maximum inhibition efficiencies of the targeted inhibitors varied between 84.52 and 95.36% at the concentration (1.0 mM). The extracted data in the table shows that with increasing PABITC concentrations, the cathodic Tafel slope values (βc) decreased more than the anodic Tafel slope values (βa), compared to free solution. The cathodic Tafel slope βc variations suggest that PABITC influences the hydrogen evolution kinetics [17, 18]. The small change in the anodic Tafel slope values (βa) with increasing PABITC concentration indicates that these compounds do not change the iron dissolution mechanism.

It is clear from Table 3, the presence of PABITC in the corrosive medium shift's corrosion potential (E_{corr}) of the studied C- steel in the positive direction of about 50 mV compared to E_{corr} in the free aggressive solution. This result indicates that the inhibitor affects the anodic process more than the cathodic one. These results elucidated that PABITC is a hybrid type of inhibitor (with dominant anodic effectiveness) acting on both the hydrogen evolution reaction and metal dissolution. Finally, the finding shows that PABITC could restrain the corrosion of C-steel coupon in 0.50 M H_2SO_4 solution, and a better inhibition property is seen in the case of PABITC (P4).

3.4.Adsorption isotherm

The mechanism of organic molecule adsorption on the surface of the C- steel is considered as a substitution adsorption process between both the organic compound in the aqueous phase (Org_{aq}) and the water molecules adsorbed on the C-steel surface (H_2O_{ads}) [43]:

$$Org_{aq} + x\ H_2O \longrightarrow Org_{ads} + x\ H_2O_{aq} \qquad [9]$$

where x is the size ratio of the water molecules quantity replaced by an adsorbate molecule. At equilibrium, different adsorption isotherms plots were tested. The experimental results obtained from Weight loss measurements at '25 °C' fit well Langmuir adsorption isotherm thermodynamic model (see Fig (7)) [43]. Langmuir adsorption isotherms were represented by the following equation:

$$\frac{C_{inh}}{\theta} = \frac{1}{K_{ads}} + C_{inh} \qquad [10]$$

K is the binding constant of the adsorption reaction and C_{inh} is the inhibitor concentration in corrosive solution. *K* can be associated to the standard free energy of adsorption ΔG°_{ads} via the following

equation: $$K_{\text{ads}} = \left(\frac{1}{c_{\text{solvent}}}\right).e^{\frac{-\Delta G_{\text{ads}}}{RT}} \qquad [11]$$

where *R* is the universal gas constant, *T* is the absolute temperature, and $C_{solvent}$ is the concentration of water in solution.

The calculated values are given in Table 4. As is evident from the table, the adsorbed layer on the steel surface is thermodynamically stable as the addition of the **PABITC** causes $K_{ads} > 1$. The calculated negative values of ΔG_{ads}, according to equation [11], indicated that adsorption of studied **PABITC** is a spontaneous process [44, 45]. Generally, values of ΔG_{ads} are defined to indicate both physisorption and chemisorption. Where values up to -20 kJ. mol^{-1} refers to physisorption that is associated with electrostatic interaction between both the charged molecules and the charged metal. Whilst these about -40 or more kJ. mol^{-1} is related to chemisorption arising from electron sharing or transfer from the inhibitor molecules to the metal surface to form a coordination bond. The calculated ΔG_{ads} value approximately ranging from -34.03 to -38.47 **kJ. mol^{-1}** indicates, therefore, that the adsorption mechanism of the **PABITC** on C- steel in 0.50 **M** H_2SO_4 were both electrostatic-adsorption and chemisorption [46].

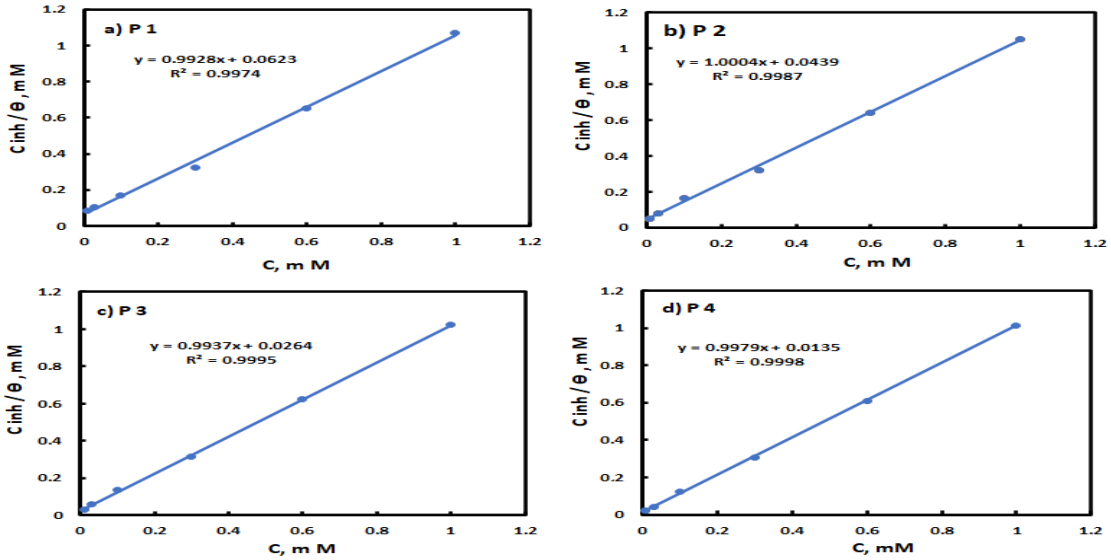

Figure 7: Langmuir adsorption plots for carbon steel in 0.5 M H_2SO_4 in absence and the presence of different concentrations of of diverse concentrations of different M w s of PABITC at 298 K.

Table 4: Thermodynamic parameters of adsorption for C- steel in 0.5 M H_2SO_4 containing different concentrations of different **Mws** of **PABITC** at 298 ***K***.

Paramters	**P1**	**P2**	**P3**	**P4**
$1/K_{ads}$ (M^{-1})	6.2 x 10^{-5}	4.4 x 10^{-5}	2.6 x 10^{-5}	1.4 x10^{-5}
ΔG_{ads}(kJ.mol^{-1})	- 34.036	-35.040	-35.750	-38.474

3.5.Morphological study approach

3.5a. Scanning electron microscopy (SEM*)*

The given SEM images in Fig. 8 (a- d) illustrate the impact of 1.0 mM **PABITC** addition on the morphological structure of C-steel specimens after 12 h immersion time. Fig. 8a represents the SEM image of the C- steel specimen after immersion in 0.5 M free sulphuric acid, where the sample shows a highly corroded surface and deep pits. However, in presence of optimum concentrations of polymers Fig. 8 (b- d),

Figure 8: Surface morphologies of C- steel after immersion in 0.50 M H2SO4 solution a) without inhibitor, (b) with 1.0 mM P1 inhibitor, C) with 1.0 mM P3 inhibitor and (d) with 1.0 mM P4 inhibitor for 12 h at 298 K.

the SEM micrographs exhibit a very significant variation in the surface morphologies. Increasing the surface softness in presence of **PABITC** is endorsed the formation of protective polymers film on the C- steel by adsorption on the metallic surfaces.

3.5b: Energy dispersive X- ray spectroscopy (EDX)

The adsorption of the PABITC on metallic surface was also confirmed by Energy Dispersive X- ray spectroscopic analysis. EDX analysis was done to ascertain the presence of the elements on the electrode surface after immersing in acid solutions with and without PABITC. The EDX spectrum of steel in 0.50 M H_2SO_4 shows characteristic peaks of iron (Fe), carbon (C) and oxygen (O) (Fig 9.a).

As clear in the absence of PABITC, the EDX spectrum shows characteristic signals for oxygen on the C- steel surface and that may be attributed to the formation of ferrous and ferric oxide as a result of atmospheric oxidation of iron during SEM/EDX analyses [43]. while that of C- steel immersed in PABITC solution (Fig 9 b-d) exhibits two more signals related to N and S, which assures that the PABITCs molecules involved in bonding with C- steel electrode surface through these atoms. Moreover, the peak of O -atom is decreased significantly comparing with that in the absence of PABITC which endorse that the PABITC form a protective film on C- steel surface.

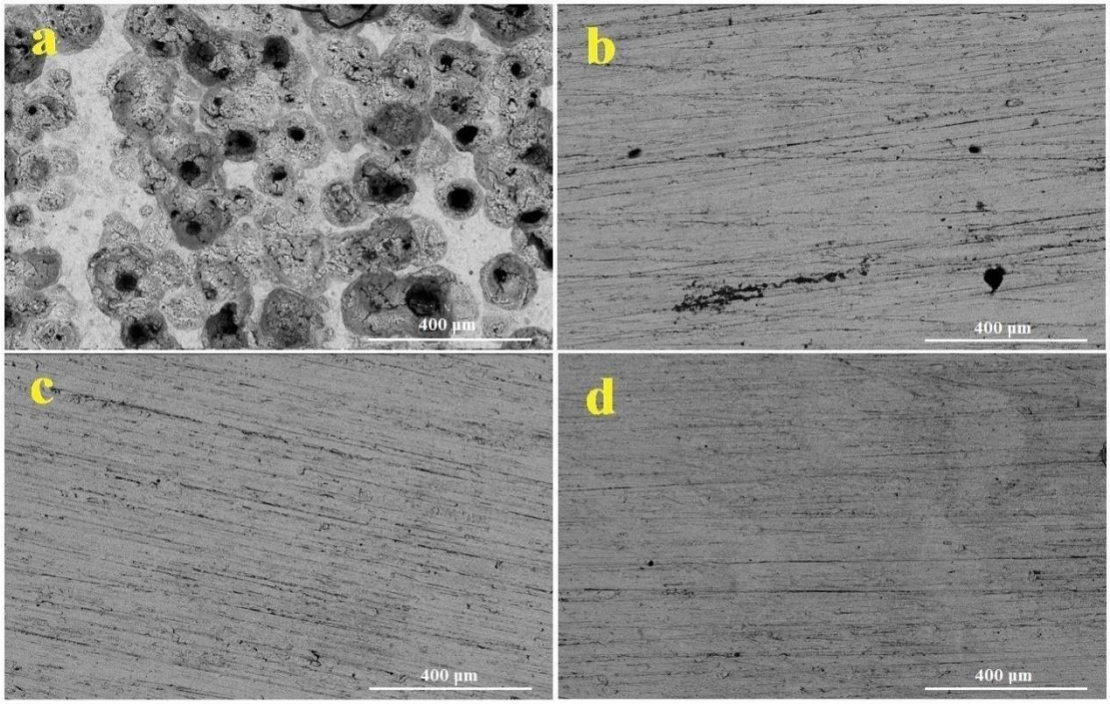

Figure 8: Surface morphologies of C- steel after immersion in 0.50 M H_2SO_4 solution a) without inhibitor, (b) with 1.0 mM P1 inhibitor, C) with 1.0 mM P3 inhibitor and (d) with 1.0 mM P4 inhibitor for 12 h at 298 K.

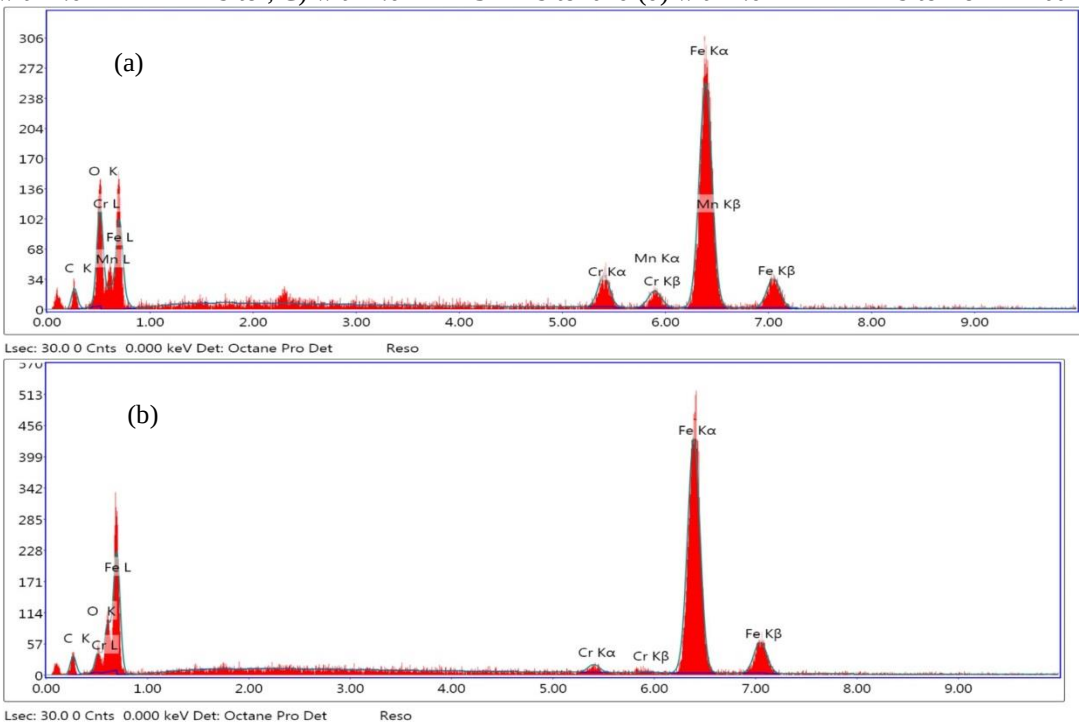

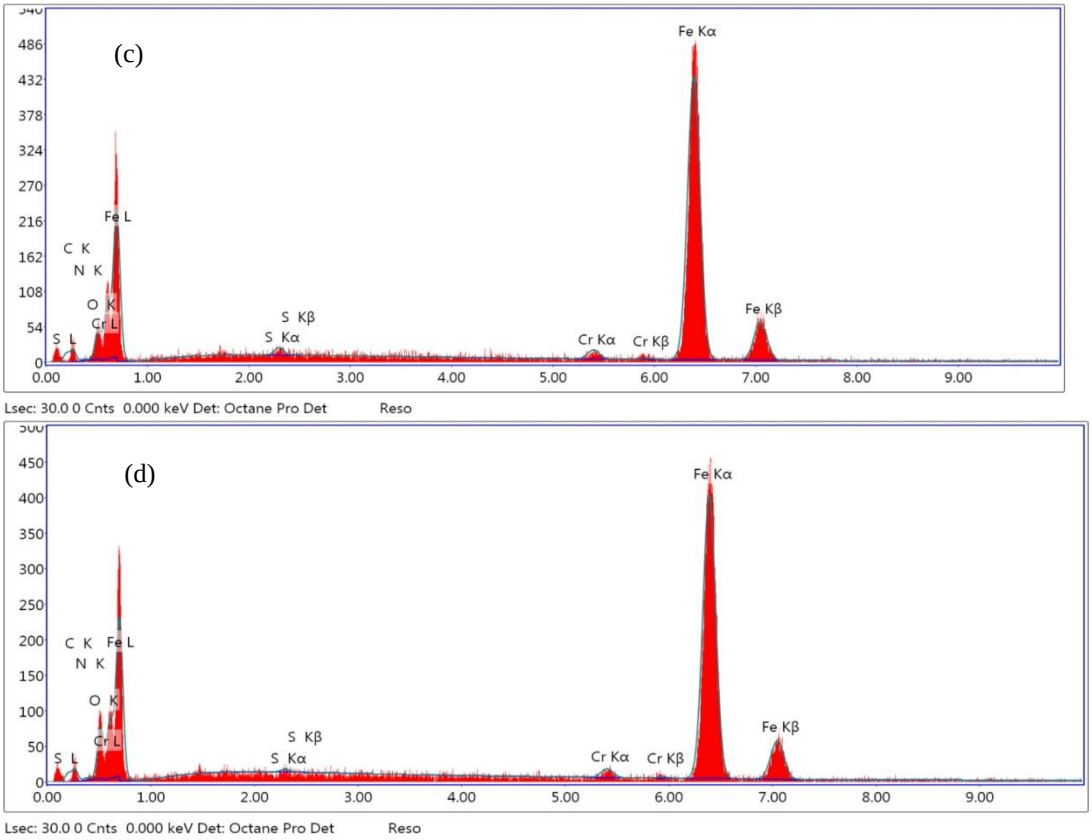

Figure 9: EDX spectra of C- steel in0.50 M H_2SO_4 solution a) without inhibitor, (b) with 1.0 mM P1 inhibitor, C) with 1.0 mM P3 inhibitor and (d) with 1.0 mM P4 inhibitor for 12 h at 298 K.

3.6.Quantum Chemical Calculation

The optimized geometry structure and the density distribution of frontier molecular orbitals (HOMO and LUMO) of PABITC are shown in Fig. 10. Obviously, HOMO is distributed through the whole molecular skeleton, indicating that the favored inhibitor`s electrophilic attack sites would be the heteroatoms of both thiophene and indole rings, amine group, a cyano group, and the benzene ring as well. On the other side, the LUMO orbitals of PABITC, which can admit electrons from the metal via Л*orbitals to generate Л-back bonds, are overfilled around the rings and seemingly delocalized. In other words, the value of EHOMO of a molecule defines the capability to donate its HOMO electrons to the corresponding acceptor molecule, whilst the value of ELUMO determines the susceptibility of the molecule to accept electrons into its LUMO from a suitable donor [43, 45].

Some calculated chemical quantum parameters influence the inhibitor's electronic interaction with the C- steel surface tabulated in Table 5. The table reveals a high value of E_{HOMO} and a low value of E_{LUMO} that, in turn, leads the polymer molecules to share electrons with the C- steel easily, indicating a strongly inhibitive action. The low value of the energy gap designates the behavior of PABITC molecules towards the C-steel. It maximizes the ability to restrain corrosion and achieves high inhibitive performance [43-46]. Consequently, the required energy for removing the electrons in HOMO of the PABITC into Fe 3d-orbital has a minimum value. Moreover, the minimum value of E_{LUMO} allows the inhibitor to gain electrons from the filled Fe 3d orbital [47, 48] or the filled Fe 4s orbital [49, 50].

If $\Delta N < 0$: the electrons are moved from Fe surface to inhibitor molecule. If $\Delta N > 0$: the electrons are transferred from the inhibitor molecule to the Fe surface [51, 52]. Here, the calculated $\Delta N > 0$ indicating to a strong tendency for the electrons transfer from the PABITC molecules to C- steel surface. Both chemical hardness (η) and softness (σ) are associating with the selectivity and reactivity of the molecule. η measures the resistance of an atom or to a charge transfer. The small calculated value of η indicates that the polymer reacts more easily with the C- steel surface, where the corrosion action decreases [53, 54].

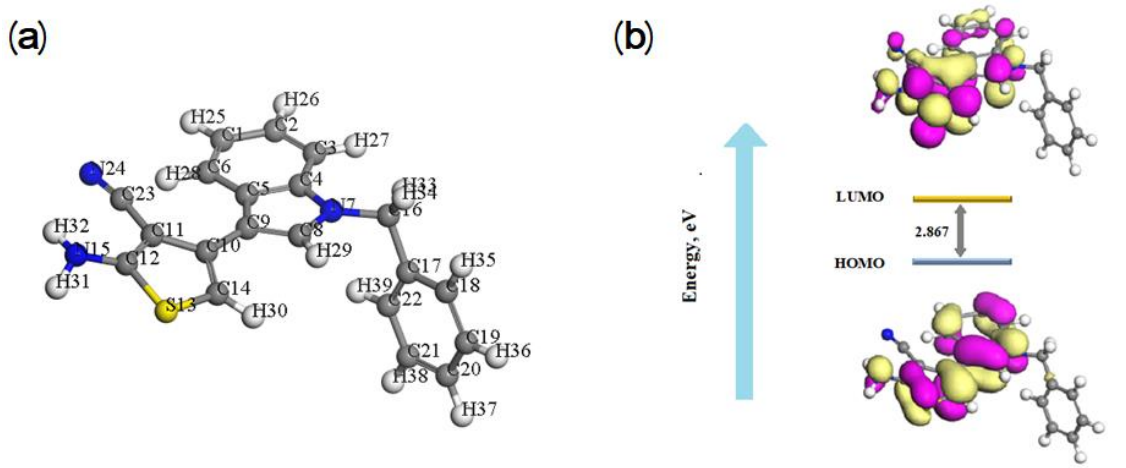

Figure 10: (a) Optimized structure, (b) molecular orbital HOMO and LUMO, respectively for PABITC**.**

Table 5: Calculated quantum chemical parameters of PABIT

Inhibitor	E_{HOMO}, eV	E_{LUMO}, eV	ΔE, eV	η	σ, eV^{-1}	μ, Debye	χ, eV	ΔN_{max}
PABITC	**– 4.097**	**–1.230**	**2.867**	**1.4335**	**0.3754**	**-2.6635**	**2.6635**	**1.85804**

The electronegativity (χ) demonstrates the electron attracting ability of the inhibitor molecule. Therefore, the high value of χ_{inh} indicates the high inhibitor strength to accept electrons from the iron surface and maintains strong interaction with the metallic surface atoms that leads to a high *IE*%.

Additionally, the low dipole moment (μ) of PABITC molecules favors a better accumulation of molecules around the surface layer and supports high inhibition efficiency [55-58].

3.7. Mechanism of the C- steel corrosion and its inhibition

The corrosion of C- steel in sulfuric acid is occurred according to [59]:

The anodic dissolution:

$$Fe + H^+ + e^- \Rightarrow FeH \quad [12]$$

$$FeH + FeH \Rightarrow 2\,Fe + H_2 \uparrow \quad [13]$$

$$H_2O_{ads} \Rightarrow OH^-_{ads} + H^+_{aq} \quad [14]$$

$$Fe + OH^-_{ads} \Leftrightarrow Fe(OH)_{ads} + e^- \quad [15]$$

$$Fe(OH)_{ads} \Rightarrow FeOH^+ + e^- \quad [16]$$

$$FeOH^+ + H^+ \Leftrightarrow Fe^{2+} + H_2O \quad [17]$$

The cathodic hydrogen evolution follows;

$$Fe + H^+_{ads} \Leftrightarrow FeH^+_{ads} \quad [18]$$

$$FeH^+_{ads} + e^- \Leftrightarrow FeH_{ads} \quad [19]$$

$$FeH_{ads} + H^+ + e^- \Leftrightarrow Fe + H_2\uparrow \quad [20]$$

corrosion process of Fe in acidic sulfate solutions is occurred by the dissolution of Fe and hydrogen evolution reactions. Where the C- steel surface contain positive ions on the anodic sites and iron atoms at the cathodic sites. In the absence of the PABITC, occur attraction of water molecules as ligand in both the anodic and cathodic sites through the partial negative charge on oxygen of the water or possible co- ordination bond of lone pair on the oxygen.

In a sulfuric acid medium, the C- steel surface is positively charged where the values for Antropov's rational corrosion potential, $E_r = E_{Corr} - E_{PZC}$, is electropositively charged due to the oxidation of iron and the presence of an excess of H_3O^+ [60].

The corrosion of C- steel in H_2SO_4 solutions in the existance of PABITC molecules as inhibitor decreases efficiently. The obtained higher inhibition efficiencies can be explained by strong adsorption of the PABITC molecules on the surface of C- steel so, such adsorption may be physical, chemical, or a mixture of both with various amplitudes. In an acidic medium, the presence of the fabricated PABITC molecules is anticipated to protonate and /or neutral on the positively C- steel surface. so two processes of adsorption take place.

The mechanism of inhibition can be proposed as follow [61], the adsorption of a PABITC species from aquatic medium is a quasi-replacement process, in which a PABITC species in the aquatic phase replaces an X number of H_2O molecules adsorbed on the C- steel interface as follows [62]:

$$PABITC_{sol} + X\,H_2O_{ads} \Rightarrow PABITC_{ads} + X\,H_2O_{sol} \quad (21)$$

It is known that the molecular structure of the inhibitor, the density of surface charge, and the potential of zero charges of metal (E pzc) affect on the adsorption efficiency of PABITC on the metallic surface. The two processes of adsorption can be explained as follow:

(i) The neutral inhibitor PABITC molecules have numerous lone pairs of electron localized at its active sites (for ex; p- electrons of N and/ or S

atoms and π electron's of phenol) which stabilize the electrically positive iron surface through interactions with its unoccupied d- orbitals. Coordinated bonds are established and chemical adsorption occurs. This interaction is supported by back donation of the valance s- and / or d – electrons of the C- steel surface to the LUMO orbitals of the PABITC.

Therefore, PABITC molecules may be overlapped with the freshly Fe ions (Eq. 22) on the steel surface, building a metal–organic inhibitor complex:

$$\textbf{PABITC}_{\textbf{ads}} + \textbf{Fe}^{2+} \Rightarrow \textbf{Fe}^{2+}\textbf{ - PABITC}_{\textbf{ads}} \quad \textbf{(22)}$$

The resulting complex, **[Fe^{2+}–polymer]** $_{ads}$, could protect the metal surface, and (ii) The formed overlap between the protonated PABITC molecules with the sulfate ions facilitates their adsorption on the metal surface via a simple electrostatic mechanism. Thence, there is a fraternize between the adsorbed sulfate ions and the protonated PABITC, therefore, replacing the water molecules. In addition, sulfate anions, SO_4^{2-}, adsorbed by electrostatic interaction to the positively charged C- steel surface. The formed FeSO4 known as barely soluble and adheres more efficiently to the C- steel surface. In both those case, physical adsorption occurs. Produced iron compounds and examined PABITC molecules are considered as an Impenetrable passive protective layer leading to shifting the iron corrosion potential towards positive values. Similar mechanisms have been previously reported for different corrosion inhibitors [63]**.** In other words, the earlier data support that PABITC adsorption occurs via polar groups such phenols, N, and S where functional groups supersede H_2O and H_3O^+ at the steel surface.The hydrophobic part of the **PABITC** molecules forms a protective film that decreases the access of the corrosive solution to the steel surface. **T**hrough comparison at a constant concentration of **PABITC**, the differences of inhibitive action between the **PABITC** of different molecular weight **[Table (2)]** were attributed to: the hydrophobic chain length present in the studied polymers; besides increasing [2-amino-4(1-benzyl-1H-indol-3-yl) thiophene-3-carbonitrile)] unit of the adsorbed polymer on the metal surface increases the number of = C- S, amino group –NH, and π electrons of phenol which have high electronegativity giving the polymer molecules the chance to form chemisorption on the C- steel surface [64-66]. These two effects make the surface more hydrophobic and the metal surface becomes more effective protective layer against corrosive attack in 0.50 M H_2SO_4, leading to increasing IE %.

3.8. Conclusion

The PABITC, has been synthesized and inspected for their inhibition performances on C- steel corrosion in 0.5 M H_2SO_4 solution. The results of both gravimetric and electrochemical experiments showed that all PABITC with different *M*w inhibits C- steel corrosion in 0.5 M H_2SO_4 solution and the inhibition efficiency increases with increasing concentration of the inhibitor. The adsorption of studied PABITC subjects the Langmuir isotherm and involves competitive physisorption and chemisorption modes. Potentiodynamic polarization studies showed that the PABITC inhibits both anodic and cathodic half-reactions associated with the corrosion process. Surface morphology studies using SEM / EDX provided some evidence of the formation of the protective film of PABITC on the steel surface. The experimental and surface morphology studies confirmed that the inhibition performances of the PABITC is found to have the following descending order: $P_4 > P_3 > P_2 > P_1$ due to increase number of repeating ABITC unit. The increase in the inhibition potential was attributed to increasing molecular size/volume of the molecule, which corresponds to increase in surface coverage. Quantum calculations elucidate that the reactive sites in PABITC are N and S atoms with the π cloud of aromatic rings.

Acknowledgement

The authors are thankful to Dr. Sahar M. Ibrahim for her fruitful cooperation and assistance in carrying out the Quantum chemical studies.

Conflict of interest

The authors declare there is no conflict of interest, financial, or otherwise.

Author Contributions

The manuscript was written through contributions of all authors. All authors have given approval to the final version of the manuscript.

References

1. Quraishi M A 2017 Journal of the Association of Arab Universities for Basic and Applied Sciences **23** 29
2. Abd El-Lateef H M 2015 Corrosion Science **92** 104
3. Mohana K N and Tandon H C 2018 Arab Journal of Basic and Applied Sciences **25** 45

4. Kumar C B PMohana K N and Muralidhara H B 2015 Ionics **21** 263
5. Tan JGuo L and Xu S 2015 Journal of Industrial and Engineering Chemistry **25** 295
6. Finšgar M and Jackson J 2014 Corrosion Science **86** 17
7. Ansari K RChauhan D SSingh ASaji V S and Quraishi M A,2020 *Corrosion Inhibitors for Acidizing Process in Oil and Gas Sectors*, in *Corrosion Inhibitors in the Oil and Gas Industry*. p. 151.
8. Rostami A.2009 *SPE International Symposium on Oilfield Chemistry*.
9. Rajeev PSurendranathan A and Murthy C S 2012 J. Mater. Environ. Sci **3** 856
10. Palanisamy G, 2019 *Corrosion inhibitors*. Intechopen London.
11. Obot I B and Edouk U M 2017 Journal of Molecular Liquids **246** 66
12. Sathiyanarayanan SMarikkannu C and Palaniswamy N 2005 Applied Surface Science **241** 477
13. Verma C BQuraishi M and Singh A 2015 Journal of the Taiwan Institute of Chemical Engineers **49** 229
14. Yadav MKumar SSharma U and Yadav P 2013 J. Mater. Environ. Sci **4** 691
15. Aljourani JRaeissi K and Golozar M A 2009 Corrosion Science **51** 1836
16. Torres V V, Amado R S, de Sá C F, Fernandez T L, Riehl C A d S, Torres A G, and D'Elia E 2011 Corrosion Science **53** 2385
17. Deshpande P PJadhav N GGelling V J and Sazou D 2014 Journal of Coatings Technology and Research **11** 473
18. Rohwerder M 2009 International Journal of Materials Research **100** 1331
19. Döşlü S TMert B D and Yazıcı B 2013 Corrosion Science **66** 51
20. Tüken TDüdükçü MYazıcı B and Erbil M 2004 Progress in Organic Coatings **50** 273
21. Ocón PCristobal A BHerrasti P and Fatas E 2005 Corrosion Science **47** 649
22. Zhang Y, Shao Y, Liu X, Shi C, Wang Y, Meng Get alYang Y 2017 Progress in Organic Coatings **111** 240
23. Abdel Hakim A.A. A Z G, Nasar Mona, A.F.Shaaban, Rasha Abdel Baseer *Preparation of some epoxy primers modified with nano polyaniline composite, and their applications in the field of metallic packaging*, in *4th International Conference of Chemical Industries Research Division*. 2010: Cairo.
24. Sambyal PRuhi GDhawan R and Dhawan S K 2016 Surface and Coatings Technology **303** 362
25. Gopi DKarthikeyan PKavitha L and Surendiran M 2015 Applied Surface Science **357** 122
26. Pruna A and Pilan L 2012 Composites Part B: Engineering **43** 3251
27. Döşlü S TDoğru Mert B and Yazıcı B 2018 Arabian Journal of Chemistry **11** 1
28. El-Sawy E R, Mandour, A. H., Mahmoud, N. A. , Abo-Salem, H. M 2012 Egyptian Journal of Chemistry **55** 239
29. Mndzhoyan APapayan GZhuruli LKaragezyan SGalstyan L and Sarafyan V 1969 Arm. Khim. Zh.(USSR) **22** 707
30. ASTM, *Standard Practice for Laboratory Immersion Corrosion Testing of Metals*. 1990, ASTM: Philadelphia, PA. p. 401.
31. Corrales Luna MLe Manh TCabrera Sierra RMedina Flores J VLartundo Rojas L and Arce Estrada E M 2019 Journal of Molecular Liquids **289** 111106
32. Singh AQuraishi M and Ebenso E E 2012 Int. J. Electrochem. Sci **7** 12545
33. Gómez BLikhanova N VDomínguez-Aguilar M AMartínez-Palou RVela A and Gázquez J L 2006 The Journal of Physical Chemistry B **110** 8928
34. Pearson R G 1963 Journal of the American Chemical Society **85** 3533
35. Pearson R G 1988 Inorganic Chemistry **27** 734
36. Kokalj A 2012 Chemical Physics **393** 1
37. Kovačević N and Kokalj A 2011 The Journal of Physical Chemistry C **115** 24189
38. Tan JGuo L and Xu S 2015 Journal of Industrial and Engineering Chemistry **25** 295
39. Kovačević N and Kokalj A 2011 Corrosion Science **53** 909
40. Sundberg R J, 1970 *The Chemistry of the Indoles*. New York: Academic Press.
41. Baseer R AAbd-Rabou A AZarie E SAzouz R A M and Abo-Salem H 2020 Egyptian Journal of Chemistry **64** 235
42. Gopi DSaraswathy RKavitha L and Kim D K 2014 Polymer International **63** 280
43. Kaczerewska OLeiva-Garcia RAkid R and Brycki B 2017 Journal of Molecular Liquids **247** 6
44. Obot I BMacdonald D D and Gasem Z M 2015 Corrosion Science **99** 1
45. Saha S KDutta AGhosh PSukul D and Banerjee P 2016 Physical Chemistry Chemical Physics **18** 17898
46. Javadian SDarbasizadeh BYousefi AEktefa FDalir N and Kakemam J 2017 Journal of the Taiwan Institute of Chemical Engineers **71** 344
47. Khaled K 2009 Journal of Solid State Electrochemistry **13** 1743
48. Oguzie EEnenebeaku CAkalezi COkoro SAyuk A and Ejike E 2010 Journal of Colloid and interface Science **349** 283
49. Heakal F E-TFouda A and Zahran S 2015 Int. J. Electrochem. Sci **10** 1595

50. Li YZhao PLiang Q and Hou B 2005 Applied Surface Science **252** 1245
51. El Ibrahimi B, Soumoue A, Jmiai A, Bourzi H, Oukhrib R, El Mouaden Ket alBazzi L 2016 Journal of Molecular Structure **1125** 93
52. Kovačević N and Kokalj A 2011 Corrosion Science **53** 909
53. El Sayed HEl Nemr AEsawy S A and Ragab S 2006 Electrochimica Acta **51** 3957
54. Zarrouk A, Hammouti B, Dafali A, Bouachrine M, Zarrok H, Boukhris S, and Al-Deyab S S 2014 Journal of Saudi Chemical Society **18** 450
55. Al-Azawi K F, Mohammed I M, Al-Baghdadi S B, Salman T A, Issa H A, Al-Amiery A Aet alKadhum A A H 2018 Results in Physics **9** 278
56. Murulana L CKabanda M M and Ebenso E E 2015 RSC Advances **5** 28743
57. Rochdi A, Kassou O, Dkhireche N, Touir R, El Bakri M, Touhami M Eet alHammouti B 2014 Corrosion Science **80** 442
58. Yousef TEl-Reash G A and El Morshedy R 2013 Journal of Molecular Structure **1045** 145
59. Fawzy AFarghaly T ABahir A A AHameed A MAlharbi A and El-Ossaily Y A 2021 Journal of Molecular Structure **1223** 129318
60. Khalaf M MTantawy A HSoliman K A and Abd El-Lateef H M 2020 Journal of Molecular Structure **1203** 127442
61. Kokalj A 2010 Electrochimica Acta **56** 745
62. El-Awady A AAbd-El-Nabey B A and Aziz S G 1992 Journal of the Electrochemical Society **139** 2149
63. Chung I-MMalathy RPriyadharshini RHemapriya VKim S-H and Prabakaran M 2020 Materials Today Communications **25** 101687
64. Daoud DDouadi TIssaadi S and Chafaa S 2014 Corrosion Science **79** 50
65. Quartarone GBonaldo L and Tortato C 2006 Applied Surface Science **252** 8251
66. Chauhan L R and Gunasekaran G 2007 Corrosion Science **49** 1143